Contribution from the Department of Chemistry,
The Ohio State University, Columbus, Ohio 43210

Metal–Metal Bonding in Dirhodium Tetracarboxylates. Structure of the Bis(diethylamine) Adduct of Tetra-μ-acetato-dirhodium(II) and Systematics of the Bonding in Tetracarboxylate-Bridged Metal Dimers

Y. B. KOH and G. G. CHRISTOPH*

Received November 16, 1978

The structure of the bis(diethylamine) adduct of dirhodium tetraacetate has been analyzed by X-ray crystallography and the results are compared with those for the structures of the diaquo and bis(pyridine) adducts. The Rh–Rh bond, at 2.4020 (7) Å, is greater than in the bis(pyridine) complex and 0.0165 (9) Å greater than in the diaquo complex, in accord with the ranked σ-donor abilities of these ligands. The Rh–N bond is about 0.2 Å longer than expected for mononuclear Rh(I) or Rh(III) complexes, consistent with the very strong Rh–Rh bond. The tetraacetate framework of the diethylamine adduct is very similar to that of the other adducts. Examination of the bonding parameters of more than 40 tetracarboxylate-bridged metal dimers reveals that, despite differences in the R group of the carboxylate and differences in the metals, the M–M–O angle is a remarkably linear function of the M–M distance. The O–C–O angles for each R depend linearly upon the M–M distance, and the slope of O–C–O vs. M–M is characteristic of R, decreasing in the order H $\gg$ CH_3 $\sim$ Ph > CF_3. The M–O–C angles appear to be the most flexible of the interbond angles, adjusting to accommodate the requirements of both the particular R group and the particular M–M distance. The O–C–O angles and C–O bond lengths for the dirhodium tetraacetates are found to be anomalous when compared with those of the other tetraacetate-bridged complexes. The tetraacetate framework could without difficulty accommodate a much longer Rh–Rh distance than is observed, suggesting that the bridging acetates do not constrain the Rh–Rh distance to be 0.3 Å less than expected for a single Rh–Rh bond. Bis(diethylamine)tetra-μ-acetato-dirhodium(II) crystallizes with four molecules per unit cell in the orthorhombic space group *Pbcn*. The molecule possesses a crystallographic center of symmetry. The cell constants are a = 16.329 (4) Å, b = 8.011 (4) Å, and c = 17.660 (6) Å for λ(Mo K$\bar{\alpha}$) 0.71069 Å. Data were collected by automated diffractometer and corrected for Lorentz–polarization and absorption effects. The structure was solved by the heavy-atom Patterson method and refined by convential Fourier least-squares techniques to a final R factor of 0.066 for 3346 unique reflections.

Introduction

The carboxylate-bridged transition-metal dimers $M_2(O_2CR)_4L_2$, I, demonstrate the full range of direct metal–metal

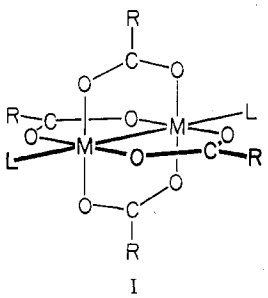

I

interactions, from very weak to exceptionally strong, and the description and understanding of the bonding in these complexes have proven to be both difficult and stimulating.[1] Despite the intense interest in such compounds, as evidenced by the large number of structural investigations of complexes where M = Mo(II), Cr(II), and Cu(II), a number of challenging problems remain; among them is the question of the extent of involvement of the bridging carboxylate groups in determining the equilibrium metal–metal distance and consequently their role in influencing the degree of the metal–metal interactions. While the range of metal–metal distances that can be accommodated by the tetracarboxylate cage is quite large (2.0–2.8 Å), the metal–metal distances for a given metal generally fall only in a fairly narrow range peculiar to that metal. The metal–metal distances for a few metals, such as Mo(II) and Re(III), correlate well with those found in dimeric complexes lacking bridging ligands, which suggests that it is the metal–metal interactions alone which determine the M–M internuclear separation. For others, however, encapsulation in the tetracarboxylate framework leads to unusually short metal–metal distances. This is in particular true for M = Rh(II). The extraordinarily short (2.386 Å) Rh–Rh bond in $Rh_2(OAc)_4(H_2O)_2$ prompted the initial assignment by Cotton and co-workers of the metal–metal bond as triple,[2] in comparison with the much longer (2.936 Å) Rh–Rh bond, which was formulated as single, in the non-bridged dimer complex $Rh_2(dmg)_4(PPh_3)_2$.[3] Subsequently, Dubicki and Martin concluded that the spectral behavior of $Rh_2(OAc)_4L_2$ complexes was more consistent with formulation of the Rh–Rh bond as single.[4] This viewpoint has more recently found substantial support in the SCF–Xα–SW calculations of Norman and Kolari on the $Rh_2(O_2CH)_4$ and $Rh_2(O_2CH)_4(H_2O)_2$ systems,[5a] and an EPR study of a nitroxide adduct of $Rh_2(O_2CCF_3)_4$ has been reported whose results are consistent with the single-bond formulation.[5b]

The abnormally short Rh–Rh distance in these bridged complexes has led us to undertake a systematic study of the effects of varying the base strength of the axial ligands upon the Rh–Rh bond. We have previously reported the results of the structure analysis of $Rh_2(OAc)_4(py)_2$.[6] We report here the details of the crystal structure of $Rh_2(OAc)_4(NHEt_2)_2$ and discuss these in the context of the general structural features of the tetra-μ-carboxylato framework.

Experimental Section

Synthesis and Characterization. Single crystals of $Rh_2(OAc)_4(NHEt_2)_2$ were obtained by slow evaporation at room temperature of the solvent after dissolving a small amount of $Rh_2(OAc)_4(CH_3OH)_2$ (prepared by a literature method[7]) in neat $NHEt_2$. The crystals were dark red needles soluble in most hydrocarbon solvents, but they reverted to a green material, presumably $Rh_2(OAc)_4(H_2O)_2$, on evaporation of the solvents (e.g., cyclohexane, benzene, toluene). The axial ligands were readily displaced by solvent molecules containing oxygen atoms (e.g., MeOH, DMF, H_2O). $RhCl_3 \cdot 3H_2O$ was purchased from Alfa Inorganics and all of the reagents were used as received, without further purification.

IR (KBr pellet, Perkin-Elmer 457 grating IR spectrophotometer, range 4000–250 cm^{-1}): 3281 (w), 2980 (sh), 2962 (m), 2935 (w), 2883 (m), 1595 (s), 1487 (sh), 1428 (s), 1360 (w), 1346 (m), 1145 (w), 1121 (m), 1068 (w), 1048 (m), 1039 (m), 935 (m), 916 (w), 840 (m), 817 (w), 790 (w), 703 (s), 629 (m), 590 (w), 511 (w), 435 (w), 380 (s), 348 (w), 336 (m) cm^{-1}.

UV–vis (neat $NHEt_2$; Cary 15, range 300–700 nm): λ_{max} 540 nm (ϵ 196 ± 31 M^{-1} cm^{-1}).

X-ray Data Collection. A cleaved portion of a needle crystal was coated with a thin layer of epoxy and mounted with (001) parallel to the goniometer axis. The dimensions were approximately 0.33 × 0.24 × 0.32 mm. Preliminary precession photographs showed systematic absences consistent with the orthorhombic space group *Pbcn*:

0020-1669/79/1318-1122$01.00/0

$0kl$, $k = 2n + 1$, $h0l$, $l = 2n + 1$, and $hk0$, $h + k = 2n + 1$. The lattice constants and their standard deviations were determined from a least-squares analysis of the optimized diffractometer setting angles of 15 reflections for which $7.0 < 2\theta < 23.0°$; $a = 16.329$ (4) Å, $b = 8.011$ (4) Å, $c = 17.660$ (6) Å, $V = 2310$ (1) Å^3, ρ(measd) = 1.60 g/cm^3, ρ(calcd) = 1.691 g/cm^3, λ(Mo K$\bar{\alpha}$) 0.71069 Å, $t = 20$ (1) °C. The density could not be measured accurately due to dissolution or decomposition of the crystals in all solvents employed. The value given above was obtained by flotation in a mixture of bromobenzene and iodobenzene. The linear absorption coefficient for Mo K$\bar{\alpha}$ radiation was 14.31 cm^{-1}.

A total of 5042 intensities in the range $4.0° < 2\theta < 60.0°$ were collected (Syntex $P\bar{1}$ automated diffractometer) at 20 ± 1 °C by the θ–2θ scan technique using graphite-monochromatized Mo K$\bar{\alpha}$ (λ 0.71069 Å) radiation. A variable scan speed was employed: 2.0°/min for reflections with less than 200 counts during a preliminary 2-s intensity measurement and 24.0°/min for those with more than 2000 counts. Backgrounds were measured by the fixed crystal–fixed counter method for one-quarter of the total scan time at each end of the scans. The intensities of seven standard reflections were remeasured after every 93 reflections and they showed no sign of crystal decay. The intensity data were placed on an absolute scale by means of a Wilson plot[8] and corrected for Lorentz and polarization effects. ψ scan intensities for each of 13 independent reflections near $\chi = 90.0°$ remained constant to within ±7% from their mean values. The absorption corrections were applied using

$$I_{obsd} = I_{cor}(a_0 + \sum_{i=1}^{n} a_i f_i(\theta_p,\phi_p))(a_0' + \sum_{i=1}^{n} a_i' f_i(\theta_s,\phi_s))$$

where θ_p and ϕ_p are the angles of the incident beam and θ_s and ϕ_s are those of the diffracted beam relative to the crystal coordinates. The coefficients were determined by an iterative nonlinear least-squares procedure utilizing the ψ scan data. The elimination of the systematically absent reflections and the averaging of the multiply measured reflections resulted in 3346 unique data, all of which were used in the structure determination and refinement. Of these, 2081 reflections had intensities greater than three standard deviations above the background.

The estimated variances in the observations were calculated using

$$\sigma^2(F_o^2) = R(S + T^2(B_1 + B_2) + (pI)^2)$$

where R is the scan rate, S, B_1, and B_2 are the total scan and individual background counts, T accounts for the relative times spent counting scan or backgrounds, I is $S - T(B_1 + B_2)$, and p is taken to be 0.02.[10]

Structure Determination and Refinement

The phase problem was solved by the heavy-atom method. Carbon, nitrogen, and oxygen coordinates were deduced from Fourier and difference Fourier maps. Four cycles of isotropic refinement by full-matrix least squares gave

$$R = \frac{\sum||F_o| - |F_c||}{\sum|kF_o|} = 0.11$$

and

$$R_w = \left\{\frac{\sum(w^2(|kF_o|^2 - |F_c|^2)^2)}{\sum(w^2|kF_o|^4)}\right\}^{1/2} = 0.20$$

The refinement was continued with anisotropic thermal parameters for atoms having no hydrogen atoms. A difference synthesis showed residual peaks with intensities of as high as 0.90 e/Å^3 around C(5), C(6), C(7), and C(8). Some were chosen as probable hydrogen atom positions, but none of them refined to convergence. Attempts to locate hydrogen atoms on N, C(2), and C(4) were also unsuccessful. The hydrogen atoms were given $B = 6.0$ Å^2 and assigned to the most probable positions in tetrahedral environments at a distance of 0.95 Å from the carbon atoms to which they were attached.

Several cycles of anisotropic least-squares refinement resulted in convergence at $R = 0.066$ and $R_w = 0.099$. All final shifts were less than one-fifth of their estimated standard deviations at the conclusion of the refinement. The goodness of fit, $[w(F_o^2 - F_c^2)^2/(n_o - n_p)]^{1/2}$, was 2.10 for $n_o = 3346$ and $n_p = 126$. The maximum and minimum peaks in the final difference map were 1.75 e/Å^3 and −1.26 e/Å^3, associated with C(5) and C(8), respectively. The general noise level was ±0.40 e/Å^3.

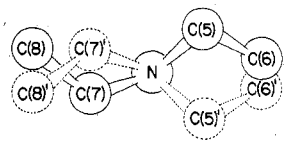

Figure 1. Possible orientation–conformation disorder of the diethylamine ligand, viewed down the N–Rh axis.

Disorder of the carbon atoms of the $NHEt_2$ group was evident in the bond distances involving these atoms and in the shape and size of their thermal ellipsoids. The distances are shorter by 0.05–0.18 Å than the expected values for the corresponding single C–N and C–C bonds, and the vibration amplitudes for C(5), C(6), C(7), and C(8) were unreasonably large (maximum ~0.5 Å). A difference map calculated without the disordered carbon atoms showed severe dispersion of the electron density, especially for C(5) and C(7), in directions roughly perpendicular to the Rh–N axis. The disorder was judged to be a mixture of the two possible configurations of the $NHEt_2$ group in one or more rotational orientations of the amine and of the ethyl groups, as shown in Figure 1. Attempts were made to resolve the disorder by creating two half-weighted (isotropic) carbon atoms near the ends of the major ellipsoid axis of each carbon atom. The least-squares refinement of the coordinates of the half-weighted carbon atoms diverged, and this approach was abandoned. As is apparent in the packing diagram (Figure 3), the ethyl groups make closest approaches to the acetate methyl groups on neighboring molecules. The disorder of the former is certainly the origin of our inability to reliably locate the hydrogen atoms of the latter.

The function minimized in the full-matrix least-squares refinement was of the form

$$w(k^2F_o^2 - F_c^2)^2$$

where k is a scale factor and the weights $w = \sigma^{-2}(F_o^2)$. The scattering factors for O, N, and C were taken from ref 11a and that for Rh from ref 11b. The form factor for Rh was corrected for the real component of anomalous dispersion using the values given in ref 11b. The form factor of H was that of Stewart, Davidson, and Simpson.[12]

The absorption corrections were calculated using the locally written EMPPSI, an empirical absorption program that used ψ scan data.[9] The modified CRYM crystallographic computing system was used for all other computations.[13] Table I lists the final values of all of the refined parameters with the estimated standard deviations as obtained from the final least-squares cycle.

Results

Bond distances and angles for the nonhydrogen atoms are listed in Tables II and III. Table IV gives the least-squares planes with their direction cosines and deviations of individual atoms from the planes.

The geometry of the tetra-μ-acetatodirhodium nucleus (Figure 2) is very similar to that found in the diaquo[2] and bis(pyridine)[6] adducts. There are, however, small but significant differences. The Rh–Rh distance is 2.4020 (7) Å, which is 0.0057 (9) Å greater than in the bis(pyridine) adduct and 0.0165 (9) Å greater than in the diaquo adduct. The changes in the tetraacetate framework accompanying the increased metal–metal distances are small, and, although by themselves only barely significant, suggestive of a trend in how the framework accommodates various metal–metal distances (vide infra). The rhodium atoms are displaced 0.07 Å out of the plane of their equatorial oxygen donors toward the axial ligands. The Rh–Rh–N linkage is not quite linear, being 176.2°. The Rh–N bond is approximately 0.2 Å longer than expected, on the basis of covalent radii for N and Rh(I) or Rh(III) or in comparison with literature values.[14]

The amine group is far from being planar, as is shown by the substantial deviations of the atoms from the least-squares plane based upon the positions averaged by the disorder. This suggests that the orientations of the $NHEt_2$ groups in Figure 1 are of unequal population. Although this assures us that the $NHEt_2$ groups are pyramidal (the amine hydrogen atoms could not be located), the C–N–C angle is too unreliable to

Table I

Fractional Coordinates ($\times 10^5$) and Anisotropic Thermal Parameters ($\times 10^4$) of $Rh_2(OAc)_4(NHEt_2)_2$[a]

atom	x	y	z	U_{11}	U_{22}	U_{33}	U_{12}	U_{13}	U_{23}	equiv iso B, Å²
Rh	3 736 (2)	6 749 (4)	−4 993 (2)	355 (2)	469 (2)	404 (2)	−28 (2)	29 (2)	8 (2)	3.23
N	11 233 (26)	18 181 (51)	−14 733 (27)	810 (28)	585 (26)	705 (29)	−85 (23)	319 (27)	48 (25)	5.53
O(1)	−6 285 (16)	21 634 (38)	−6 637 (18)	435 (15)	531 (17)	560 (20)	8 (14)	20 (14)	69 (16)	4.02
O(2)	13 227 (17)	−8 906 (37)	−2 792 (18)	413 (15)	602 (19)	558 (19)	24 (14)	32 (15)	67 (17)	4.14
O(3)	−1 167 (18)	−10 197 (37)	−12 274 (18)	545 (16)	591 (20)	461 (18)	−67 (16)	26 (16)	−26 (16)	4.20
O(4)	8 212 (17)	22 855 (39)	2 935 (17)	458 (15)	571 (19)	489 (19)	−110 (15)	14 (14)	0 (16)	4.00
C(1)	−12 448 (25)	19 271 (54)	−2 486 (27)	429 (21)	507 (25)	512 (26)	8 (21)	−23 (21)	−16 (23)	3.81
C(2)	−19 928 (25)	29 991 (64)	−4 182 (32)	459 (24)	817 (34)	943 (43)	179 (25)	−51 (29)	219 (35)	5.84
C(3)	6 004 (24)	21 044 (59)	9 801 (28)	408 (21)	516 (25)	529 (27)	−25 (20)	−23 (20)	−76 (24)	3.82
C(4)	9 424 (30)	32 941 (62)	15 476 (32)	776 (34)	665 (32)	645 (33)	−93 (28)	4 (30)	−201 (30)	5.49
C(5)	10 132 (68)	34 414 (98)	−16 612 (57)	3263 (128)	777 (50)	1666 (89)	−96 (72)	1637 (96)	56 (57)	15.02
C(6)	10 129 (43)	47 507 (83)	−12 074 (44)	1264 (58)	811 (45)	1109 (61)	18 (44)	210 (53)	18 (44)	8.38
C(7)	13 205 (44)	5 969 (91)	−20 490 (39)	1217 (56)	1339 (57)	930 (51)	−359 (50)	560 (46)	−219 (53)	9.18
C(8)	19 298 (40)	8 799 (97)	−26 409 (40)	1215 (53)	1573 (65)	895 (51)	2 (55)	317 (50)	−226 (56)	9.69

Fractional Coordinates ($\times 10^3$) of Hydrogen Atoms[b]

atom	x	y	z	B, Å²	atom	x	y	z	B, Å²
H(21)	250	150	70	6.0	H(62)	140	480	−95	6.0
H(22)	250	250	20	6.0	H(63)	92	600	−140	6.0
H(23)	310	110	30	6.0	H(71)	83	21	−225	6.0
H(41)	60	374	200	6.0	H(72)	152	−14	−167	6.0
H(42)	150	260	170	6.0	H(81)	150	170	−280	6.0
H(43)	110	430	125	6.0	H(82)	220	110	−230	6.0
H(51)	47	345	−190	6.0	H(83)	170	0	−310	6.0
H(52)	140	367	−205	6.0	H(1)	170	210	−160	6.0
H(61)	50	490	−95	6.0					

[a] The form of the anisotropic temperature factor is $\exp[-2\pi^2(U_{11}h^2a^{*2} + \ldots + 2U_{23}klb^*c^*)]$. The equivalent isotropic B has been calculated from the magnitudes of the principal-axis amplitudes of the thermal ellipses. [b] Not refined.

Table II

Bond Distances of $Rh_2(OAc)_4(NHEt_2)_2$ with Estimated Standard Deviations (Å)

Rh–Rh′	2.4020 (7)	O(3)–C(3′)	1.253 (5)
Rh–O(1)	2.046 (3)	O(4)–C(3)	1.273 (6)
Rh–O(2)	2.031 (3)	C(1)–C(2)	1.523 (6)
Rh–O(3)	2.034 (3)	C(3)–C(4)	1.492 (7)
Rh–O(4)	2.038 (3)	C(5)[a]–C(6)[a]	1.320 (11)
Rh–N	2.301 (5)	C(7)[a]–C(8)[a]	1.461 (10)
O(1)–C(1)	1.259 (5)	N–C(5)[a]	1.354 (9)
O(2)–C(1′)	1.255 (6)	N–C(7)[a]	1.447 (9)

Average Distances of Equivalent Bonds with Estimated Standard Deviations (Å)

Rh–O	2.038 (3)	C–CH_3	1.508 (7)
O–C	1.260 (6)		

[a] Disordered atoms; these errors are grossly underestimated.

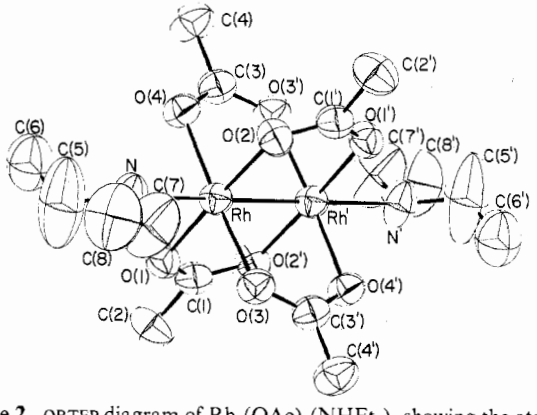

Figure 2. ORTEP diagram of $Rh_2(OAc)_4(NHEt_2)_2$ showing the atomic numbering scheme and the thermal motions (ellipsoids drawn at the 50% level).

estimate the degree of hybridization of the nitrogen atom. The high *apparent* thermal motions of the ethyl groups likewise preclude assessment of the intermolecular interactions of these

Table III

Bond Angles of $Rh_2(OAc)_4(NHEt_2)_2$ with Estimated Standard Deviations (deg)[a]

Rh′–Rh–N	176.6 (1)	N–Rh–O(1)	95.0 (1)
Rh′–Rh–O(1)	87.7 (1)	N–Rh–O(2)	89.0 (1)
Rh′–Rh–O(2)	88.2 (1)	N–Rh–O(3)	90.2 (1)
Rh′–Rh–O(3)	87.9 (1)	N–Rh–O(4)	94.1 (1)
Rh′–Rh–O(4)	87.9 (1)	O(1)–C(1)–O(2′)	127.8 (3)
Rh–O(1)–C(1)	118.0 (3)	O(3)–C(3)–O(4′)	126.1 (4)
Rh–O(2)–C(1′)	118.3 (3)	O(1)–C(1)–C(2)	116.2 (4)
Rh–O(3)–C(3′)	119.4 (3)	O(2′)–C(1)–C(2)	116.0 (4)
Rh–O(4)–C(3)	118.7 (3)	O(4)–C(3)–C(4)	117.5 (4)
O(1)–Rh–O(2)	175.9 (1)	O(3′)–C(3)–C(4)	116.4 (4)
O(3)–Rh–O(4)	175.8 (1)	Rh–N–C(5)[b]	119.7 (5)
O(1)–Rh–O(3)	89.2 (1)	Rh–N–C(7)[b]	112.0 (4)
O(1)–Rh–O(4)	90.9 (1)	C(5)[b]–N–C(7)[b]	120.4 (6)
O(2)–Rh–O(3)	90.5 (1)	N–C(5)[b]–C(6)[b]	127.9 (9)
O(2)–Rh–O(4)	89.2 (1)	N–C(7)[b]–C(8)[b]	123.3 (6)

Average Angles of Equivalent Bonds with Estimated Standard Deviations (deg)[a]

Rh′–Rh–O	87.9 (1)	O–C–O	127.0 (4)
Rh–O–C	118.6 (3)		

[a] The esd's tabulated are as calculated from the inverted matrix from the final least-squares cycle. For the disordered atoms the esd's grossly underestimate the true errors, which are likely about 6–10°. [b] Disordered atoms.

atoms, although the C(4)···C(6) contact appears to be the most significant. All nonbonded contacts involving atoms not in the $NHEt_2$ ligands are normal (Table V and Figure 3).

Discussion

As shown in Table VI, the Rh–Rh bond distance increases slightly, but significantly, with the increasing σ-donor strengths of H_2O, py, and $NHEt_2$ (pK_b's, respectively, 15.7, 8.75, and 3.51[15]). Carbon monoxide, a comparatively weak σ-donor but effective π-acceptor ligand, yields a longer Rh–Rh distance, its greater trans-influence effect presumably the result of stronger net Rh–L interactions. Curiously, the relative stabilities of these complexes are in the order L = py ≈ H_2O >

Table IV

Least-Squares Planes

plane	devs (Å) from planes	direction cosines		
A	Rh,[a] 0.074; O(1), 0.001; O(2), 0.001; O(3), −0.001; O(4), −0.001	0.5047	0.4533	−0.7347
B	Rh, −0.013; Rh, −0.016; O(1), 0.020; O(2′), 0.025; C(1), 0.017; C(2), −0.033	0.3525	0.6705	0.6528
C	Rh, −0.001; Rh, −0.004; O(4), 0.004; O(3′), 0.007; C(3), 0.000; C(4), −0.005	−0.7727	0.6145	−0.1593
D	N, −0.156; C(5),[b] 0.266; C(6),[b] −0.128; C(7),[b] 0.105; C(8),[b] −0.087	−0.8143	0.0647	−0.5769

Dihedral Angles, Deg

planes	angle	planes	angle
A-D	93 (6)	C-D	40 (2)
B-D	51 (3)	B-C	92 (2)

[a] The rhodium atom was given a weight of zero in the least-squres calculation. [b] Disordered atoms.

Table V. Nonbonded Intermolecular Distances (Å) Less Than 4.0 Å[a]

O(4)-C(2) (iv)	3.583 (5)	C(2)-C(8)[b] (iii)	3.826 (9)
C(4)-C(6)[b] (v)	3.607 (9)	O(3)-C(7)[b] (iii)	3.848 (8)
C(3)-C(6)[b] (v)	3.667 (8)	O(3)-C(6)[b] (i)	3.858 (7)
C(1)-C(6)[b] (v)	3.720 (9)	O(3)-C(8)[b] (iii)	3.883 (8)
C(2)-C(6)[b] (v)	3.749 (9)	O(2)-C(6)[b] (i)	3.891 (8)
O(2)-C(2) (iv)	3.801 (6)	C(2)-C(4) (v)	3.967 (7)
O(1)-C(8)[b] (iii)	3.812 (8)	O(1)-C(4) (v)	3.993 (6)
C(4)-C(8)[b] (ii)	3.816 (8)		

[a] Symmetry list: (i) $x, 1+y, z$; (ii) $^1/_2-x, {}^1/_2-y, -{}^1/_2+z$; (iii) $-x, y, -{}^1/_2-z$; (iv) $-{}^1/_2+x, {}^1/_2-y, -z$; (v) $-x, 1-y, -z$. [b] Disordered atoms.

$NHEt_2 > CO$. The CO complex is unstable both in the solid state and in solution, decomposing in the latter completely within 20 min at room temperature to free CO and unsubstituted $Rh_2(OAc)_4$.[16] As noted above, the $NHEt_2$ adduct is also labile, the axial ligand being easily displaced by solvents possessing oxygen donor atoms. In neat hydrocarbon solvents it reverts to unsubstituted $Rh_2(OAc)_4$ upon evaporation of the solution. If care is not taken to exclude water vapor, some or all $Rh_2(OAc)_4(H_2O)_2$ results. The bis(pyridine) complex, on the other hand, shows signs of decomposition only when *heated* in H_2O, DMF, MeOH, or like solvents, forming, by displacement, complexes of the form $Rh_2(OAc)_4(solvent)_2$. These qualitative observations are in agreement with the findings of Kitchens and Bear,[17] which give a higher estimate for the heat of reaction for (1) for L = py than for $LNHEt_2$ (36.7 kcal/mol vs. 33.1 kcal/mol).

$$Rh_2(OAc)_4L_2(s) \rightarrow Rh_2(OAc)_4(s) + 2L(g) \qquad (1)$$

Although this data could be interpreted to suggest that the Rh–N(py) bond is augmented by π back-bonding, there are several serious reasons to doubt this. First, pyridine is at best a weak π acceptor, and, given the longer than normal Rh–N distance, even this capacity must be substantially reduced in the dirhodium complex. Second, the trans influence, as measured by the Rh–Rh distance, is greater for $NHEt_2$, which is not a π acceptor, and greater still for CO, which is a good π acceptor. Since the trans influence of a ligand is directly related to the strength of the metal–ligand interaction, the Rh–CO bond should be, despite its greater lability, stronger than the Rh–$NHEt_2$ bond, which in turn should be stronger than the Rh–N(py) bond. For L = H_2O, py, and $NHEt_2$ the Rh–Rh distance is almost a linear function of the pK_b's; if Rh–N(py) π interactions were important, then the Rh–Rh distance should not be a function only of the ligand σ-donor strength. Third, the observed reaction enthalpies cannot be taken as absolute or unambiguous measures of the Rh–N bond strenghts both because of unknown lattice or solvation energy contributions and, more seriously, because of the increase in the Rh–Rh bond energy when it shortens on dissociation of the axial ligand. Since the thermochemical measurements reflect the net resultant of these several contributions, the various adducts can even be thermally unstable relative to the dissociated components but still possess reasonably strong Rh–Rh and Rh–L bonds. It is the *coupling* of the bond-energy changes upon making or breaking the Rh–L bond that most likely accounts for the observed order of stabilities of the adducts.

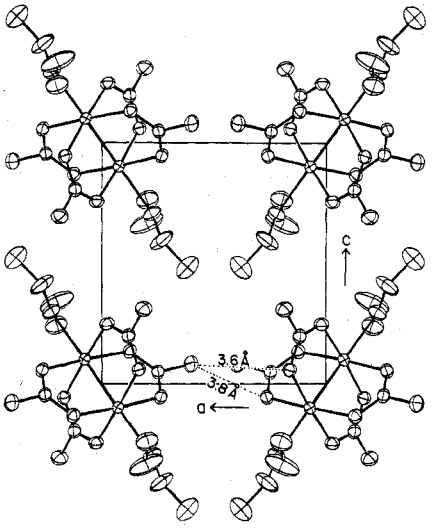

Figure 3. Packing diagram. Projection of unit cell contents onto the *xz* plane.

The large number of tetracarboxylate-bridged metal dimers that have been studied structurally have prompted us to consider the systematics of changes in the geometry of the framework when the metal–metal distance is varied. The relevant data are assembled in Table VII, except for the dirhodium complexes, which appear in Table VI. The range of metal–metal distances that can be accommodated by the tetracarboxylate framework is surprisingly large—nearly 0.75 Å. Before we discuss the trends in the bridging acetate geometry for the dirhodium complexes, for which the range of

Table VI. Structural Data for $Rh_2(OAc)_4L_2$

L	*d*(M–M), Å	*d*(M–L), Å	*d*(M–O), Å	*d*(C–O), Å	M–M–O, deg	M–O–C, deg	O–C–O, deg	ref
H_2O	2.3855 (5)	2.310 (3)	2.039 (8)	1.269 (4)	88.1 (3)	119.5 (3)	124.8 (3)	2
py	2.3963 (2)	2.227 (3)	2.039 (2)	1.266 (3)	88.0 (3)	119.1 (1)	125.7 (1)	6
$NHEt_2$	2.4020 (7)	2.301 (5)	2.038 (3)	1.260 (6)	87.9 (1)	118.6 (3)	127.0 (4)	this work
CO	2.4193 (3)	2.091 (3)	2.032 (2)	1.266 (3)	87.6 (1)	119.6 (2)	125.5 (2)	16
PPh_3	2.449 (2)	2.479 (3)	2.044 (4)	1.268 (7)	87.1 (1)	118.9 (4)	126.4 (4)	24
$(NO)(NO_2)$	2.4537 (4)	1.933 (4)[a] 2.010 (4)[b]	2.026 (3)	1.270 (5)	86.0 (1)	118.8 (2)	125.5 (3)	16

[a] L = NO. [b] L = NO_2.

Table VII. Structural Data for Complexes $M_2(O_2CR)_4L_2$

compd	d(M-M), Å	d(M-L), Å	d(M-O), Å	d(C-O), Å	M-M-O, deg	M-O-C, deg	O-C-O, deg	ref
$Cu_2(O_2CH)_4(NCS^-)_2$	2.716 (2)	2.093 (9)	1.983 (4)	1.244 (8)	83.0 (1)	122.7 (3)	128.4 (3)	25
$Cr_2(O_2CH)_4(py)_2$	2.408 (1)	2.308 (3)	2.019 (3)	1.258 (5)	87.6 (2)	119.7 (4)	125.4 (3)	21
$(Cr_2(O_2CH)_4(H_2O)_2)_3\cdot 10H_2O$[e]	2.373 (2)	2.268 (4)	2.015 (4)	1.257 (8)	87.9 (1)	119.6 (4)	124.9 (6)	
	2.360 (2)	2.210 (6)	2.121 (5)	1.251 (8)	87.9 (1)	119.9 (4)	124.3 (5)	26
$Cr_3(O_2CH)_6(H_2O)_2$	2.451 (1)	2.224 (2)	2.122 (3)	1.257 (5)	87.0 (2)	120.2 (2)	125.6 (3)	21
$Mo_2(O_2CH)_4$	2.091 (2)		2.11 (2)	1.29 (2)	92.0 (4)	117 (1)	121 (1)	27
$Cu_2(OAc)_4(H_2O)_2$	2.614 (2)	2.161 (2)	1.969 (2)	1.259 (2)	84.4 (1)	123.0 (1)	124.9 (1)	28[a]
$Cu_2(OAc)_4(H_2O)_2$	2.616 (1)	2.156 (4)	1.969 (3)	1.260 (6)	84.4 (1)[j]	123.1 (3)	124.8 (4)	29[b]
$Cu_2(OAc)_4(py)_2$[c]	2.645 (3)	2.186 (8)	1.955 (8)	1.24 (2)	83.7 (4)[i]	123.4 (9)[i]	126 (1)[i]	30
$Cu_2(OAc)_4(py)_2$[d]	2.630 (3)	2.13 (1)	1.98 (1)	1.24 (2)	83.6 (3)[j]	123.4 (7)	125.1 (9)	31
$Cu_2(OAc)_4(NCS^-)_2$	2.643 (3)	2.08 (2)	2.03 (1)	1.24 (2)	84.0 (3)	123 (1)	126 (1)	25
$Cu_2(OAc)_4(quin)_2$	2.652 (2)	2.224 (6)	1.977 (5)	1.23 (1)	83.4 (2)[j]	123.6 (1)	126 (1)	32
$Cu_2(OAc)_4(pyz)_2$	2.583 (1)	2.171 (6)	1.964 (5)	1.249 (7)	84.7 (1)[j]	122.7 (4)	125.3 (6)	33
$Cr_2(OAc)_4(C_5H_{11}N)_2$	2.342 (2)	2.338 (7)	2.016 (3)	1.265 (5)	88.4 (1)	119.9 (3)	123.4 (4)	34
$Cr_2(OAc)_4$	2.288 (2)		2.011 (8)	1.261 (8)	89.0 (5)	119.5 (5)	123.1 (6)	35
$Cr_2(OAc)_4(HOAc)_2$	2.300 (1)	2.306 (3)	2.014 (3)	1.263 (5)	88.9 (1)	119.6 (3)	123.1 (4)	34
$CrMo(OAc)_4$	2.050 (1)		2.07 (1)	1.274 (9)	92.3 (8)	117.1 (4)	121.2 (7)	36
$Cr_2(OAc)_4(H_2O)_2$	2.362 (1)	2.272 (3)	2.018 (2)	1.265 (4)	88.04 (5)	120.4 (1)	123.1 (2)	2
$Mo_2(OAc)_4$	2.093 (8)		2.119 (4)	1.277 (8)	91.8 (1)	117.5 (4)	121.3 (6)	22
$Cu_2(O_2CCF_3)_4(quin)_2$	2.886 (4)	2.109 (6)	1.972 (6)	1.24 (1)	80.6 (2)	124.7 (6)	129.3 (8)	53
$Cr_2(O_2CCF_3)_4(OEt_2)_2$	2.541 (1)	2.244 (3)	2.017 (2)	1.243 (4)	85.6 (1)	120.62 (2)	127.6 (3)	21
$Mo_2(O_2CCF_3)_4$	2.090 (4)		2.06 (2)	1.26 (3)	92.1 (4)[j]	115 (2)	126.0 (2.5)	23
$Mo_2(O_2CCF_3)_4(py)_2$	2.129 (2)	2.548 (8)	2.116 (6)	1.26 (1)	91.6 (2)	115.3 (6)	126 (1)	37
$Co_2(O_2CPh)_4(quin)_2$	2.832 (2)	2.102 (8)	2.037 (7)	1.25 (1)	81.6 (2)[j]	124.5 (1)	126.4 (10)	38
$Cr_2(O_2CPh)_4(PhCO_2H)_2$	2.352 (3)	2.295 (7)	2.009 (6)	1.27 (1)	88.3 (2)	120.3 (6)	122.8 (8)	21
$Re_2(O_2CPh)_4Cl_2$	2.235 (2)	2.489 (5)	2.02 (1)	1.30 (2)	90.1 (3)	120 (1)	121.5 (1.5)	38
$Mo_2(O_2CPh)_4(diglyme)_2$	2.100 (1)	2.663 (6)	2.107 (5)	1.277 (8)	91.8 (1)	117.3 (5)	121.8 (7)	40
$Mo_2(O_2CPh)_4$	2.096 (1)		2.107 (3)	1.275 (5)	91.8 (1)	117.4 (2)	121.5 (4)	41
$Cu_2(O_2CCH_2Cl)_4(2\text{-Mepy})_2$	2.747 (3)	2.16 (1)	1.975 (9)	1.25 (2)	82.6 (3)	123.6 (8)	127.3 (13)	42
$Cu_2(O_2CCH_2^-)_4(H_2O)_2$	2.610 (1)	2.102 (7)	1.926 (7)	1.256 (10)	85.8 (1)	123.5 (11)	124.3 (9)	43
$Cu_2(2\text{-}BrPhCO_2)_4(H_2O)_2$	2.624 (7)	2.17 (2)	1.99 (3)	1.26 (3)	84.3 (7)	123 (2)	124 (3)	44
$Cu_2(C_9H_7O_4)_4$	2.617 (3)	2.241 (8)	1.962 (8)	1.26 (1)	84.5 (3)[i]	122.8 (7)	125.5 (10)	45
$Cu_2(O_2CEt)_4(py)_2$	2.631 (2)	2.15 (1)	1.96 (1)	1.25 (2)	83.9 (2)[j]	122.8 (8)[j]	127 (1)	46
$Cu_2(O_2CEt)_4(3\text{-Mepy})_2$	2.6312 (4)	2.167 (2)	1.971 (2)	1.25 (4)	83.5 (1)[j]	123.3 (2)[j]	125.4 (3)	47
$Cu_2(O_2CEt)_4(dioxane)_2$	2.5634 (4)	2.227 (2)	1.953 (2)	1.257 (4)	85.12 (4)[j]	122.3 (2)[j]	125.1 (3)	48
$Cu_2(O_2CCCl_3)_4(2\text{-}ClC_5H_4N)_2$	2.766 (3)	2.145 (5)	1.957 (5)	1.230 (7)	81.9 (1)	123.8 (4)	128.4 (6)	49
$Cu_2(O_2CCH_2Cl)_4(quin)_2$	2.724 (2)	2.211 (7)	1.974 (6)	1.24 (1)	82.9 (2)	123.9 (1)	128 (1)	32
$Cr_2(O_2CC_{14}H_9)_4(DME)$	2.283 (2)	2.283 (5)	2.116 (4)	1.263 (8)	89.2 (1)	118.9 (4)	123.5 (6)	21
$Cr_2(O_2CCMe_3)_4$	2.388 (4)		2.02 (1)	1.26 (2)	87.4 (4)	120 (1)	125 (2)	21
$Mo_2(O_2CCH_2NH_3)_4(SO_4)_2(H_2O)_4$	2.115 (1)		2.125 (4)	1.26 (1)	91.6 (2)	116.4 (5)	124.0 (3)	50
$Mo_2(O_2CCMe_3)_4$	2.088 (1)		2.112 (6)	1.28 (1)	91.9 (2)	117.4 (3)	121.4 (8)	41
$Re_2(O_2CC_3H_7)_4(ReO_4)_2$	2.251 (2)	2.18 (3)	2.02 (3)	1.29 (6)	89.7 (9)	119 (3)	123 (4)	51
$Mo_2(O_2CCMe_3)_4\cdot CH_3CN$	2.194 (2)	3.054 (2)[f]	2.064 (13)[f]	*h*	90.7 (4)	*h*	*h*	52
		2.71 (2)[g]	2.081 (13)[g]					

[a] Neutron diffraction method. [b] X-ray method. [c] Orthorhombic. [d] Monoclinic. [e] Two independent molecules in one asymmetric unit. [f] M = W. [g] M = Mo. [h] Unavailable. [i] Errors are estimated from σ's of coordinates. [j] Calculated from the coordinates.

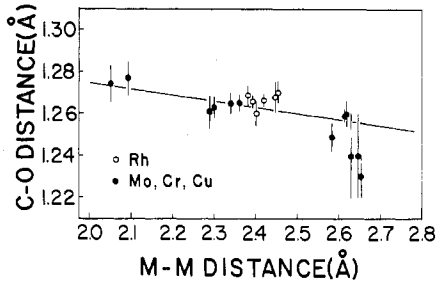

Figure 4. Carboxylate C-O distance as a function of M-M distance for Mo(II), Cr(II), Cu(II), and Rh(II) tetraacetates. The equation of the least-squares lines is $d(CO) = -0.029(9)[d(M\text{-}M)] + 1.33(2)$. The correlation coefficient $R = -0.691$. The error bars indicate $\pm 1\sigma$.

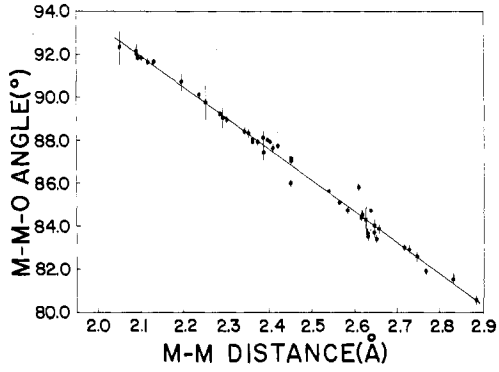

Figure 5. Variation of the M-M-O angle with M-M distance for the carboxylate-bridged complexes in Table VII. The equation of the least-squares line is M-M-O (deg) = $-14.43(9)[d(M\text{-}M)] + 122.2(2)$, with a correlation coefficient of $R = -0.992$; a linear function accounts for all but 0.8% of the observed variation of M-M-O. Error bars reflect $\pm 1\sigma$.

metal-metal distances is but 0.07 Å, it will be useful to first determine from the more extensive series which of the several carboxylate bond distances and angles are the most sensitive functions of the metal-metal distance. Since angle deformation is energetically less costly than bond stretching or compression, it is to be expected that the interior angles in the five-membered M-M-O-C-O rings are the most responsive to M-M length changes. The M-O and O-C distances for a given M are fairly constant, the latter showing an unexpected slight negative correlation with M-M (Figure 4). The M-M-O angles are in contrast very strongly correlated with the M-M distance; this is shown in Figure 5. Since the M-M-O-C-O rings are all essentially planar within exper-

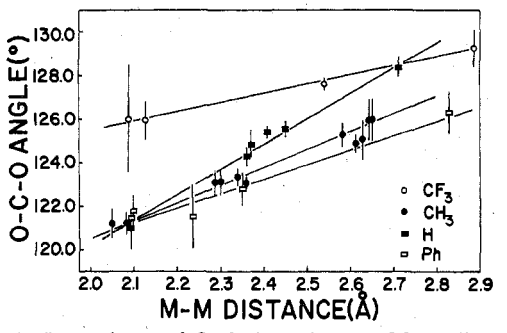

Figure 6. Dependence of O–C–O angle upon M–M distance for different carboxylate substituents. The slopes (deg/Å) [correlation coefficients in brackets] are as follows: CF_3, 4.4° [0.993]; Ph, 6.3° [0.983]; CH_3, 6.6° [0.982]; H, 11.1° [0.986]. The dirhodium tetraacetates are not included, for reasons that are apparent in Figure 7.

Table VIII. Data for Several Carboxylate Anions RCO_2^- [a]

R	pK_b [b]	O–C–O, deg	C–O, Å	O- - -O, Å	ref
CH_3	9.24	125.7 (3)	1.245 (5)	2.216	*c*
C_6H_5	9.80				
H	10.25	125.7 (2)	1.244 (3)	2.217	*d*
CF_3	13.77	128.3 (7)	1.269 (5)	2.284	*e*

[a] Structural data is for symmetric ionic salts only. [b] pK_b's taken from table in W. Hackbush, H. H. Rupp, and K. Weighardt, *J. Chem. Soc., Dalton Trans.*, 2364-2367 (1975). [c] J. L. Galigné, M. Mouvete, and J. Falgueirettes, *Acta Crystallogr., Sect. B*, **26**, 368-375 (1970). [d] Weighted means of determinations of three different salts: Enders-Buemer and S. Harkema, *ibid.*, **29**, 682-685 (1973); J. L. Galigne', *ibid.*, **27**, 2429-2430 (1971); I. Nahringhauer, *ibid.*, **24**, 565-570 (1968). [e] D. W. J. Cruickshank, D. W. Jones, and G. Walker, *J. Chem. Soc.*, 1303-1314 (1964).

imental error, this correlation requires that the sum of the O–C–O and twice the M–O–C angles will also be a linear function of the M–M distance. The correlation holds in spite of a wide variation in the nature of the R group of the carboxylic acid. The O–C–O angles by themselves, however, show interesting dependences upon the nature of R, as shown in Figure 6. Here, for a given R, the O–C–O angles increase with increasing M–M distance, but the slope, or sensitivity of O–C–O to the M–M distance, is quite characteristic of the R group. Surprisingly linear plots are obtained for the groups R = H, CH_3, Ph, and CF_3, with the slopes decreasing in the order H $\gg$ CH_3 $\sim$ Ph > CF_3. This is not the order of the base strengths for the caboxylate ligands but rather roughly the order of the size of the R group. The *magnitudes* of O–C–O angles, however, do parallel the pK_b's of the acids' conjugate bases (Table VIII). The inductive electronic effects of the R groups thus appear to be a primary factor in determining the size of the O–C–O angle. The constraints of the M–M and M–O bonds then impose secondary adjustments in the O–C–O angle, adjustments whose magnitude is governed by the "flexibility" of the O–C–O linkage. The flexibility of the carboxylate ions could, as suggested above, be a function of the steric bulk of the R group, but likely it is as well a more complex property of the sensitivity of the R group orbital overlap with the carboxylate moiety to changes in the hybridization of the central carbon atom. In this sense hydrogen may be less demanding (or more forgiving) than other R groups of the hybridization of the carboxylate carbon atom.

The plots shown in Figures 5 and 6 lead to an interesting deduction. Since for a given M–M distance the M–M–O angle can be assumed to be constant despite changes in the R group of the bridging carboxylate, it follows that changes induced in the O–C–O angle must be accommodated by compensatory changes in the M–O–C angle. Since changes in the C–O bond length with R are quite small (if anything, in a direction which exacerbates the change in O–C–O, Table IV), it is apparent that the M–O–C angles are the most flexible or the most easily deformed in response to changes elsewhere in the five-membered ring. This point is of importance in the consideration below of the dirhodium tetraacetates.

The geometry of the acetate and trifluoroacetate ligands appears to most closely approximate those of the free anions only for the long metal–metal distances of the dicopper systems. As the M–M distance decreases, the O–C–O angle becomes smaller than in the anions, and at least for the acetates (for which there are sufficient accurate data to see the effect) the C–O distance appears to lengthen concurrently. The latter may arise from strain-induced hybridization changes at the central carbon atom or from M–O interactions which cause a reduction in the C–O bond order. In any case, the longer C–O distances appear to be more characteristic of the most strongly M–M bonded systems.

The role of the carboxylate bridges in the bonding of the dirhodium tetraacetates has been controversial in that several views are possible: do the acetate bridges constrain the Rh–Rh bond to a shorter value than it would otherwise prefer, or are the rhodium atoms free to move within the framework[18] and is the geometry of the carboxylate framework accordingly readjusted in response to the bonding requirements of the Rh–Rh bond? The former view is in accord with formulation of the Rh–Rh bond as single and provides a rationale for the shortness of a bond which in the absence of bridging ligands would be closer to 2.7 Å, while the latter is consistent with a multiple Rh–Rh bond assignment. Yet a third interpretation, toward which we are inclined, is that the carboxylate bridges, perhaps through the π system, facilitate bonding interactions between the metal centers that would not occur in the absence of the bridges. Such synergistic interactions are in accord with the very strong mixing of metal and ligand atomic orbitals; the molecular orbitals in the strongly bonded Mo(II) and Cr(II) systems are extensively delocalized.[5,19] In the context of these possibilities it is now appropriate to examine the dirhodium system in comparison with the other carboxylate-bridged complexes.

It is apparent from the data in Table VII and in Figures 5 and 6 that the O–C–O and M–O–C angles are responsive to demands both of the R group substituents and of the metal–metal interactions. If we accept 2.70 Å as a reasonable value for a bona fide Rh–Rh single bond (2.76 Å according to Cotton[2,18] and 2.72 Å from Pauling radii[20]) and if we use normal Rh–O and C–O distances of 2.04 and 1.26 Å, we can construct a tetraacetate-bridged dirhodium complex having a 2.70 Å Rh–Rh distance which does not require extraordinary O–C–O and M–O–C angles. This geometry is in fact approximated by the dicopper tetraacetate systems. The observed Rh–Rh distance is more than 0.3 Å *shorter* than this, with most of the angular adjustments being taken up in the Rh–Rh–O and Rh–O–C angles. If 2.70 Å is a comfortable equilibrium internuclear Rh–Rh distance, it seems curious that the normalization of the Rh–Rh–O and Rh–O–C angles from 84 and 123° to 88 and 119°, respectively, should yield sufficient stabilization to compensate for what must surely be a repulsive part of Rh–Rh potential curve (taking 2.70 Å as the equilibrium minimum potential energy). This also contrasts sharply with the stability arguments early in our discussion which suggests that an increase in the Rh–Rh distance from 2.38 Å leads to a decrease in the Rh–Rh bond energy. We are thus left with the possibilities that the Rh–Rh bond is multiple or that the tetraacetate framework fosters additional bonding interactions which yield a much shorter equilibrium Rh–Rh distance.

The remarkable regularity of the plots in Figures 5 and 6 leads one to expect that the same relationships should hold as well for the dirhodium tetraacetates. We thus find it

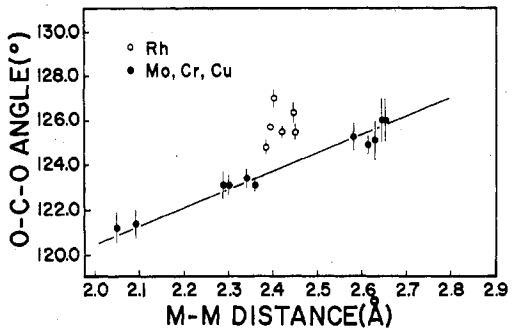

Figure 7. O–C–O angle as a function of M–M distance for tetraacetate-bridged complexes only; the dirhodium complexes deviate substantially from the other tetraacetates, suggesting some unusual rhodium–acetate interactions not present in the other complexes.

remarkable that although the Rh–Rh–O angles are in excellent agreement with the predictions of Figure 5, the O–C–O angles are exceptionally large, Figure 7, and fall far from the acetate line. The acetate C–O distances are as well larger than expected, although barely at the level of significance, but with values more characteristic of the strongly M–M bonded $Mo_2(OAc)_4X_2$ and $Cr_2(OAc)_4X_2$ systems. Consequently, the Rh–O–C angles are anomalously closer to 120° than would be predicted by any of the correlations so far discussed.

The ramifications of these observations for the order of the Rh–Rh bond are by no means clear. The data do, however, reinforce our conviction that the metal–metal and metal–carboxylate interactions in the dirhodium tetraacetates are quite strong, quite extraordinary, and quite complex.

Acknowledgment. We are grateful to The Ohio State University Instruction and Research Computation Center for a generous grant of IBM/370 computer time.

Registry No. $Rh_2(OAc)_4(NHEt_2)_2$, 69102-54-1.

Supplementary Material Available: A listing of observed and calculated structure factor amplitudes (37 pages). Ordering information is given on any current masthead page.

References and Notes

(1) F. A. Cotton, *Chem. Soc. Rev.*, **4**, 27–53 (1975); F. A. Cotton, *Acc. Chem. Res.*, **11**, 225–232 (1978); W. C. Trogler and H. B. Gray, *ibid.*, **11**, 232–239 (1978); M. Kato, H. B. Jonassen, and J. C. Fanning, *Chem. Rev.*, **64**, 99–128 (1964); P. J. Hay, J. C. Tibeault, and R. Hoffman, *J. Am. Chem. Soc.*, **97**, 4884–4899 (1975).
(2) F. A. Cotton, B. G. DeBoer, M. D. LaPrade, J. R. Pipal, and D. A. Ucko, *Acta Crystallogr., Sect. B*, **27**, 1664–1671 (1971).
(3) K. G. Caulton and F. A. Cotton, *J. Am. Chem. Soc.*, **93**, 1914–1918 (1971); M. J. Bennett, K. G. Caulton, and F. A. Cotton, *Inorg. Chem.*, **8**, 1–6 (1969).
(4) L. Dubicki and R. L. Martin, *Inorg. Chem.*, **9**, 673–675 (1970).
(5) J. G. Norman, Jr., and H. Kolari, *J. Am. Chem. Soc.*, **100**, 791–799 (1978); R M. Richman, T. C. Kuechler, S. P. Tanner, and R. S. Drago, **99**, 1055–1058 (1977).
(6) Y. B. Koh and G. G. Christoph, *Inorg. Chem.*, **17**, 2590 (1978).
(7) G. A. Rempel, P. Legzdins, H. Smith, and G. Wilkinson, *Inorg. Synth.*, **13**, 90–91 (1971).
(8) A. J. C. Wilson, *Nature (London)*, **150**, 151–152 (1942).
(9) M. A. Beno and G. G. Christoph, to be submitted for publication.
(10) W. R. Busing and H. A. Levy, *J. Chem. Phys.*, **26**, 563–568 (1957).
(11) "International Tables for X-Ray Crystallography", Kynoch Press, Birmingham, England: (a) Vol. III, 1962; (b) Vol. IV, 1974.
(12) R. F. Stewart, E. R. Davidson, and W. T. Simpson, *J. Chem. Phys.*, **42**, 3175–3187 (1965).
(13) D. J. DuChamp, "Program and Abstracts", American Crystallographic Association Meeting, Bozeman, Mont., 1965, Paper B-14.
(14) G. G. Christoph and Y. B. Koh, *J. Am. Chem. Soc.*, in press.
(15) "Handbook of Chemistry and Physics", 53rd ed., R. C. Weast, Ed., Chemical Rubber Co., Cleveland, Ohio, 1973.
(16) Y. B. Koh and G. G. Christoph, to be submitted for publication.
(17) J. Kitchens and J. L. Bear, *J. Inorg. Nucl. Chem.*, **31**, 2415–2421 (1969).
(18) F. A. Cotton and J. G. Norman, Jr., *J. Am. Chem. Soc.*, **93**, 80–84 (1971).
(19) J. G. Norman, H. J. Kolari, H. B. Gray, and W. C. Trogler, *Inorg. Chem.*, **16**, 987–993 (1977); F. A. Cotton and G. G. Stanley, *ibid.*, **16**, 2668–2671 (1977).
(20) L. Pauling, *Proc. Natl. Acad. Sci. U.S.A.*, **72**, 3799–3801 (1975).
(21) F. A. Cotton, M. W. Extine, and G. W. Rice, *Inorg. Chem.*, **17**, 176–186 (1978).
(22) F. A. Cotton, Z. C. Mester, and T. R. Webb, *Acta Crystallogr., Sect. B*, **30**, 2768–2770 (1974).
(23) F. A. Cotton and J. G. Norman, Jr., *J. Coord. Chem.*, **1**, 161–172 (1971).
(24) J. Halpern, private communication, 1977.
(25) D. M. L. Goodgame, N. J. Hill, D. F. Marsham, A. C. Skapski, M. L. Smart, and P. G. H. Troughton, *Chem. Commun.*, 629–630 (1969).
(26) F. A. Cotton and G. W. Rice, *Inorg. Chem.*, **17**, 688–692 (1978).
(27) F. A. Cotton, J. G. Norman, Jr., B. R. Stults, and T. R. Webb, *J. Coord. Chem.*, **5**, 217–223 (1976).
(28) G. M. Brown and R. Chidambaram, *Acta Crystallogr., Sect. B*, **29**, 2393–2403 (1973).
(29) P. Meester, S. R. Fletcher, and A. C. Skapski, *J. Chem. Soc., Dalton Trans.*, 2575–2578 (1973).
(30) F. Hanic, D. Stempelova, and K. Haniceva, *Acta Crystallogr.*, **17**, 633–639 (1964).
(31) G. A. Barclay and C. H. L. Kennard, *J. Chem. Soc.*, 5244–5251 (1961).
(32) Yu. A. Simonoy, V. I. Ivanov, A. V. Ablov, L. N. Milkova, and T. I. Malinovskii, *Zh. Strukt. Khim.*, **17**, 516–523 (1976).
(33) B. Morosin and R. C. Hughes, *Acta Crystallogr., Sect. B*, **31**, 762–770 (1975).
(34) F. A. Cotton and G. W. Rice, *Inorg. Chem.*, **17**, 2004–2009 (1978).
(35) F. A. Cotton, C. E. Rice, and G. W. Rice, *J. Am. Chem. Soc.*, **99**, 4704–4707 (1977).
(36) C. D. Garner, R. G. Senior, and T. J. King, *J. Am. Chem. Soc.*, **98**, 3526–3529 (1976).
(37) F. A. Cotton and J. G. Norman, Jr., *J. Am. Chem. Soc.*, **94**, 5697–5702 (1972).
(38) J. Catterick, M. B. Hursthouse, P. Thornton, and A. J. Welch, *J. Chem. Soc., Dalton Trans.*, 223–226 (1977).
(39) M. J. Bennett, W. K. Bratton, F. A. Cotton, and W. R. Robinson, *Inorg. Chem.*, **7**, 1570–1575 (1968).
(40) D. M. Collins, F. A. Cotton, and C. A. Murillo, *Inorg. Chem.*, **15**, 2950–2951 (1976).
(41) F. A. Cotton, M. Extine, and L. D. Gage, *Inorg. Chem.*, **17**, 172–176 (1978).
(42) G. Davey and F. S. Stephens, *J. Chem. Soc. A*, 2803–2805 (1970).
(43) B. H. O'Connor and E. N. Maslen, *Acta Crystallogr.*, **20**, 824–835 (1966).
(44) W. Harrison, S. Kettig, and J. Trotter, *J. Chem. Soc. A*, 1852–1856 (1972).
(45) L. Manojlovic-Muir, *Acta Crystallogr., Sect. B*, **29**, 2033–2037 (1973).
(46) M. M. Borel and A. LeClaire, *Acta Crystallogr., Sect. B*, **32**, 3333–3336 (1976).
(47) M. M. Borel and A. LeClaire, *Acta Crystallogr., Sect. B*, **32**, 1273–1275 (1976).
(48) M. M. Borel and A. LeClaire, *Acta Crystallogr., Sect. B*, **32**, 1275–1278 (1976).
(49) J. A. Moreland and R. J. Doedens, *Inorg. Chem.*, **17**, 674–678 (1978).
(50) F. A. Cotton and T. R. Webb, *Inorg. Chem.*, **15**, 68–71 (1976).
(51) C. Calvo, N. C. Jayadevan, C. J. L. Lock, and R. Restivo, *Can. J. Chem.*, **48**, 219–224 (1970).
(52) V. Katovic, J. L. Templeton, R. J. Hoxmeter, and R. E. McCarley, *J. Am. Chem. Soc.*, **97**, 5300–5302 (1975).
(53) J. A. Moreland and R. J. Doedens, *J. Am. Chem. Soc.*, **97**, 508–513 (1975).